


Innovative Calibration Strategies for Weirs with Half-Round Crest Edge Modifications

Ameer Hashim Hussein 

Al-Mussaib Technical Institute, Al-Furat Al-Awsat Technical University, Babylon 51009, Iraq

Corresponding Author Email: inm.ame@atu.edu.iq



Copyright: ©2024 The author. This article is published by IIETA and is licensed under the CC BY 4.0 license (<http://creativecommons.org/licenses/by/4.0/>).

<https://doi.org/10.18280/i2m.230502>

ABSTRACT

Received: 20 July 2024

Revised: 14 September 2024

Accepted: 27 September 2024

Available online: 25 October 2024

Keywords:

discharge coefficients, calibration methodologies, half-round edge modifications, flow patterns, rectangular weirs

This work offers a set of empirical investigations to determine the flow's discharge coefficient over rectangularity weirs via half of the crest of the circular edge extended over the entire channel width (repressed) for evaluating the flow. Three weirs were built and put through various discharge tests. They had a decent coefficient of discharge, a consistent overflow pattern, and floating debris that was easy to pass. Knowledge of the discharging head correlation for multi-models (3 models) varying weir heights (60 mm, 80 mm and 100 mm without circular edge), in addition the crest curvatures, is provided by data gathered from tests conducted in laboratories. An experimental head-discharge formula is included in every model. This study covers a crucial problem in hydraulic instrumentation and flow measurement, aligning with scientific and technical advancements in measurement and metrology. The emphasis on creative calibration procedures for modified weirs is contemporary and relevant. The anticipated flow coefficient values for the models suggested were determined using discharge-measured data and the calculated flowing formula. The examination of the findings indicated that the discharge coefficient is directly related to both the radius of curvature and the height and the upstream head above the weir crest. Empirical equations were found by multi-regression approaches with %Error (± 2 to ± 4) and Validated by the Nash-Sutcliffe model efficiency coefficient (NSE).

1. INTRODUCTION

Weirs are predominantly employed as overflow structures and for discharge measurement. The circular crested weir, the broad-crested weir, the sharp-crested weir, and the ogee crest weir are the most prevalent types of weirs. The circular crested weir is often constructed with a circle crest of a specific radius, a weir facing upstream that is opposite to the path of the incoming flow, and a weir face downstream that is about 45 degrees. In low-head dam operations, the downstream weirs' facing angle is usually fewer. The upstream flow conditions substantially impact the discharge measurements of circular weirs. The rectangular design with a half round edge weir has several advantages, featuring abilities to allow debris that floated to move through with simplicity and a consistent overflowing arrangement that contrasts sharp-crested weirs. A primary distinction between a broadly crest weir and a sharply crest weir is in the curvature of the streamlines and the more significant discharge. The curvature produces centrifugal forces or noticeable acceleration components that are normal to the flow direction [1]. The current study examines the properties of a rectangular weir with half-round edges to establish the correlation between the water level and the flow rate. The linked applications comprise three distinct designs of varnished hardwood.

The first person to methodically study the discharge coefficient (Cd) for embankment weirs was Bazin. The discharge Cd coefficient was typically closer to more

extensive than one insignificant study on circular weirs. It was also found that Cd was primarily dependent on the ratio of upstream head to crest radius H_w/R , with Cd increasing as values of H_w/R (where H_w is the total head above crest and R is the crest curvature radius) increased [2]. Johnson [3] investigated curvilinear flow in the vertical plane and causes a diversion of pressure distribution from hydrostatic. Heidarpour et al. [4] investigated curvilinear flow, which happens in the vertical plane and causes a diversion of pressure distribution from hydrostatic. Matthew [5] in 1963 proposed a formula for the discharge coefficient Cd that incorporates the influences of curvature streamlining, surface tension and viscosity. This equation allows to consider scaling effects in the hydraulic modelling of structures of the overflow. In order to study the water level, Chanson [6] inflated a rubber membrane placed across a stream or at the crest of a weir. Small overflows are typically permitted without dam deflation and resemble circular weirs in specific ways. However, these linked applications are unique fields of interest that require further investigation. While the upstream ramp had no impact on Cd, it significantly altered the upstream flow conditions due to streamlined curvature, according to experiments conducted by Chanson and Montes [7] on circular crested weir overflow with different weir radii and weir heights.

A study by Ramamurthy et al. [8] investigated the impact of weir face angles on the flow of circular-crested weirs. The investigators also calculated the weir coefficient of discharge in relation to the overall strategy flowing head. The non-

uniform velocity distribution, as demonstrated by Jalil et al. [9], is highest on the inside of the circular crested weir and lowest on the outside. In convex flow, centrifugal force acts against gravity, resulting in lower pressure than hydrostatic pressure [10, 11]. According to study of Chanson and Montes [7] and Castro-Orgaz [12], which looked at a cylindrical weir, the discharge coefficient rises with the comparative potential head and takes streamlined curvature into account. This study aims to evaluate the hydraulic characteristics of circular crested weirs with different angles on the upstream and downstream weir faces. Kumar et al. [13] proposed several different weirs with changed plan forms to increase their capacity for discharging water while maintaining a minimum head above the weirs and limiting the amount of afflux. An experimental investigation is carried out to explore the discharging capacity of sharp-crested curved plan-form weirs under free-flow circumstances in a rectangular channel. The weir height is 0.18 meters, and the vertex angles range from 45° to 120° degrees. The discharge coefficient of curved weirs has been computed using the equations that have been proposed. Based on the findings, it can be observed that a curved weir with a vertex angle of 90° exhibits an increase in discharge of approximately 40% when compared to a conventional weir.

The paper addresses an important topic in hydraulic instrumentation and flow measurement, which aligns well with the scope of scientific and technical developments in instrumentation, measurement and metrology. The focus on innovative calibration strategies for modified weirs is particularly relevant and timely. The hydraulic characteristics of the round crest weir are only dictated by the indeterminate overall upward heading H/R and are not affected by the elevation of the weir [14]. This approach will strengthen the rationale for the work and highlight its importance in advancing knowledge on discharge coefficients for weirs with half-round edge modifications. Such an expanded literature review will clarify the significance of the findings and establish a compelling basis for the need for innovation in weir design and calibration methodologies. The frequency of divergence from the pattern of hydrostatic pressure defines the local acceleration of centrifugal (V^2/r), Figure 1; hence determining the alteration of piezometric in the n -direction, as demonstrated by Hamad Mohammed [15] and Bazin [16] for two-dimensional flow patterns over cylindrical weirs as follow:

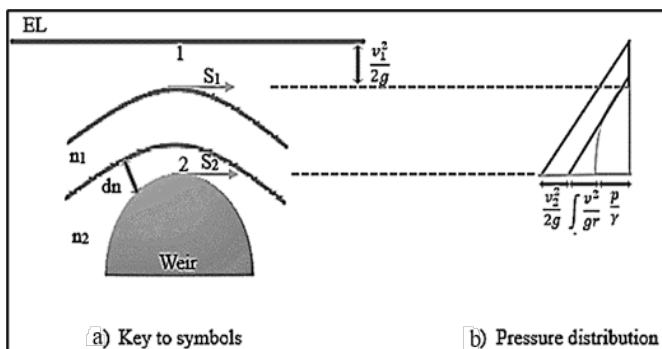


Figure 1. Convex flow

$$D \left(\frac{p}{\gamma} + Z \right) = \left(-\frac{v^2}{gr} \right) dn \quad (1)$$

Figure 1a shows the n -direction integration of the first equation from position (1) to the location (2):

$$\left(\frac{p}{\gamma} + Z \right)_1 - \left(\frac{p}{\gamma} + Z \right)_2 = \frac{1}{g} \int_1^2 \frac{v^2}{r} \cdot dn \quad (2)$$

where,

$\left(\frac{p}{\gamma} + Z \right)$: The piezometric head at a specific point;

$\frac{1}{g} \int_1^2 \frac{v^2}{r} \cdot dn$: Piezometric head losses as a result of surface line curvature.

Centrifugal acceleration causes a drop in the piezometric head, increasing the velocity head, such as:

$$\frac{v_2^2}{2g} - \frac{v_1^2}{2g} = \frac{1}{g} \int_1^2 \frac{v^2}{r} \cdot dn \quad (3)$$

2. CRITICAL DEPTH

When there is critical flow in a rectangular horizontally conduit with a pressure distribution, the flow's depth is equal to:

$$Y_c = \sqrt[3]{q^2/g} \quad (4)$$

where, Y_c is the critical depth of flow above the crest weir, L .

Despite the presence of critical flow, the pressure distribution does not follow hydrostatics. According to Salmasi et al. [17] and Alfatlawi and Hussein [18], the curvature of the streamline indicates that the pressure gradient is lower than the hydrostatic pressure gradient and that the velocity distribution is rapidly variable.

The determination of the depth of the critical and its location on a weir is primarily influenced by the effecting of friction and the curvature of streamlines. Therefore, if the flow is curvilinear ($Y_c > \frac{2}{3}y_1$), while the flow is parallel ($Y_c = \frac{2}{3}y_1$) [19, 20]. y_1 is the upstream water depth above the weir. The rectangular weir with a half-round edge is projected to have a depth different from the equation [21, 22].

3. THE PRESSURE DISTRIBUTION CALCULATION

Construction of hydraulic structures that extend beyond and where the flow has a curving nature is a crucial instance in which knowledge of the fluctuation in pressure is particularly relevant. There is a possibility that the induced pressure forces will cause damage or erosion to the face of the structure. In the vertical plane, the effect of streamlined curvature is to either enhance or decrease the distribution of pressure. The pressure decreases below hydrostatic levels when flowing over a convex surface [23, 24]. One can find the whole pressure distribution either theoretically or by empirical approaches. Experimentally information shows the pressure of average variation per unit width acting on a weir, as shown in Figure 2, $y_2 = 0.65 H_w$, the equations can be used to calculate the force that is identical to and opposed to the force imposed by the weir on a block of water:

$$P_w = \frac{\gamma y_1^2}{2} - \frac{\gamma}{2} (0.65 H_w)^2 \quad (5)$$

$$P_w = \frac{\gamma}{2} (y_1^2 - 0.42 H_w^2) \quad (6)$$

where,

P_w is a pressure per unit width ($FL^{-2}L^{-1}$);

y_1, y_2 is the upstream and downstream weir depth, respectively (L);

H_w is the water head above the weir.

The effects of streamline curvature and non-hydrostatic pressure distribution would benefit from enhanced theoretical support. Specifically, a clearer explanation of how streamline curvature affects flow patterns around the weir is essential, as it influences energy dissipation and discharge coefficients. Incorporating fundamental principles, such as Bernoulli's equation and momentum conservation.

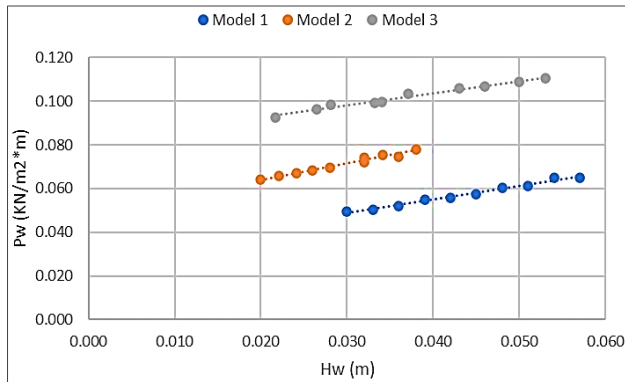


Figure 2. The relationship between the water head (H_w) and the pressure (P_w) for the three models

4. THE DISCHARGE CALCULATION

The momentum concept can be used to determine the flow per unit wide (q) of a broad crest weir over a rectangle-shaped channel. Since it solely addresses external forces operating on the weir surface, such as pressure and hydrostatic forces occurring upstream and downstream. The assumptions are that the forces caused by frictions F_f^1 and F_f^2 can be considered negligible; the first symbol represents the friction force on the bed of the channel, while the second symbol represents the friction force on the surface of a weir. Figure 3 shows the cross-section of the narrow horizontal channel, where a rectangular weir with half-round edges sits on the channel bottom and blocks the flow.

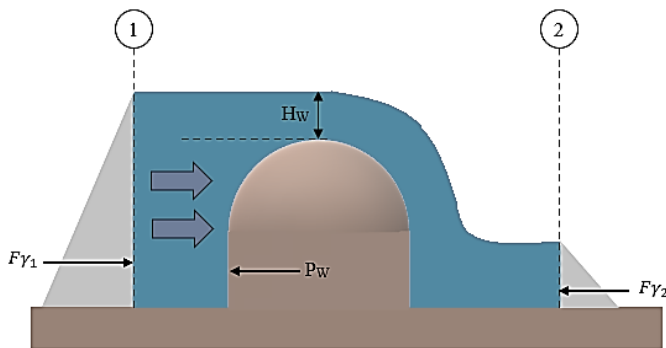


Figure 3. Outline for considering momentum in engineering

The force the weir applies to the flow is denoted by the symbol (P_w) derived from Eq. (6). If the equation for

momentum is utilized to the volume of water between the upstream approaching portion (1) and the downstream portion (2), as shown in Figure 3, the equation that follows can be derived:

$$\frac{q\gamma}{g} \left(\frac{q}{y_2} - \frac{q}{y_1} \right) = \frac{\gamma y_1^2}{2} - \frac{\gamma y_2^2}{2} - P_w \quad (7)$$

$$q_{th} = \sqrt{\frac{g}{\gamma} \left(\frac{0.65 H_w y_1}{y_1 - 0.65 H_w} \right) * \frac{\gamma y_1^2}{2} - 0.197 \gamma H_w^2 - P_w} \quad (8)$$

where,

q_{th} is the discharge theoretically per unit width ($L^3T^{-1}L^{-1}$);

g is the acceleration due to gravity (LT^{-2}).

The measured discharge is different from Formula (8) due to the presence of real-world phenomena, such as a distribution of the hydrostatic pressure and a distribution of uniform velocity, which must be considered by introducing the discharge coefficient (C_d).

5. METHODOLOGY AND EXPERIMENTAL ARRANGEMENT

The investigations were carried out at the horizontal channel with a rectangular shape (Flume) in the Fluid lab of the Babylon University, Engineering College, Civil Engineering Department, in order to estimate the discharge coefficients (C_d) for the weirs with a half-round edge. The Flume is 10 m in length (S6-Flume Tilting of zero Sloping) with a width of 30 cm and 45 cm deep. The channel's floor was stainless steel, and its acrylic walls were protected. The water depth in the Flume was measured using an Ultrasonic Water Level (UWL), as shown in Figure 4. An ultrasonic water level sensor works by emitting ultrasonic pulses toward the water surface and then measuring the time it takes for the reflected signal (echo) to return. Based on the speed of sound in the air, the sensor calculates the distance between the sensor and the water surface. The sensor emits short bursts of ultrasonic sound waves (usually above the range of human hearing, around 20 kHz to several MHz). The actual water depth can be derived by knowing the distance from the sensor to the bottom of the channel. The speed of sound in air is influenced by temperature, humidity, and pressure. Typically, the sensor compensates for temperature changes with an integrated temperature sensor.

Three models of weirs were crafted using varnished hardwood to achieve a flawless surface. The Flume is equipped with a reservoir that maintains a consistent water level. The water discharge was quantified using a Flow meter device at the start of the Flume. The flow depth was measured using a UWL sensor. Additionally, the lab examined the weir flowing using three different models with varying heights and curvature diameters, as depicted in Figure 5. These models were positioned 3.2 m upstream of the tank and were fixed directly onto the walls side (suppressed type). The flow-controlling valve was calibrated to achieve the highest achievable discharge while maintaining the equivalent upstream depth at the weir. The discharge was incrementally increased in Ten stages, with a series of measurements obtained for both (q) and (H_w) for each type of weir.



Figure 4. The Laboratory Flume: a) Pattern of flow for the Model 1; b) UWL sensor

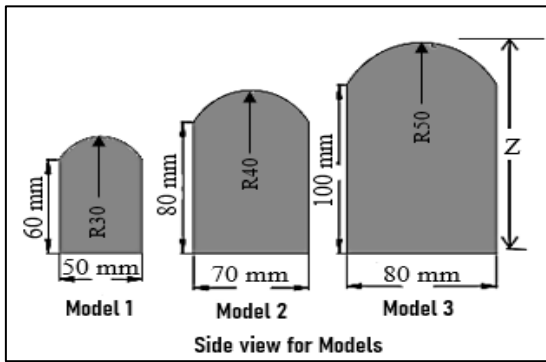


Figure 5. The weirs sketch

6. RESULTS OF APPLICATION

The difference of (q) via (H_w) for each of the three models was depicted in Figures 6, 7, 8 with the assistance of the Excel Program with a total of Ten measurements for every model. A straight-line linear relationship was found by plotting q towards H_w , which yielded its association equation:

$$q = K * H^M \quad (9)$$

The correlation experimentally for Model 1 between (H_w) via (q) with $R^2 = 99.3\%$:

$$q = 18.512 * H_w^{3.0143} \quad (10)$$

The correlation experimentally for Model 2 between (H_w) via (q) with $R^2 = 98.6\%$:

$$q = 8.471 * H_w^{2.18} \quad (11)$$

The correlation experimentally for Model 3 between (H_w) via (q) with $R^2 = 98.9\%$:

$$q = 0.2504 * H_w^{0.821} \quad (12)$$

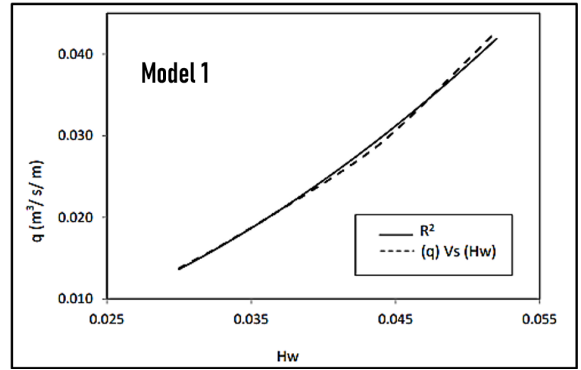


Figure 6. The relationships between the head above the crest weir and the discharge unit (Model 1)

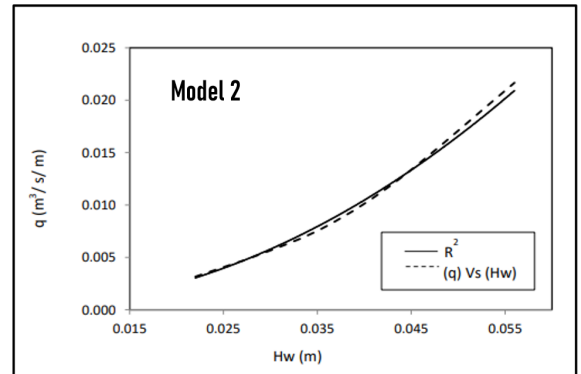


Figure 7. The relationships between the head above the crest weir and the discharge unit (Model 2)

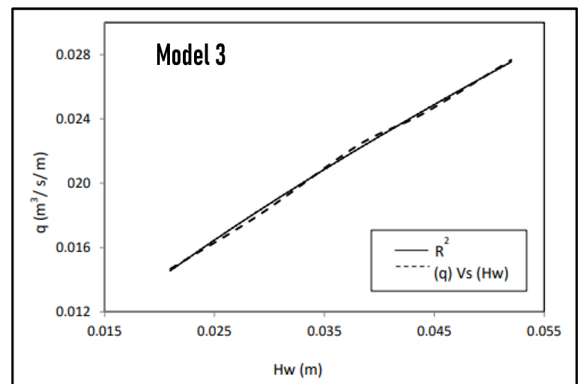


Figure 8. The relationships between the head above the crest weir and the discharge unit (Model 3)

7. THE COEFFICIENT OF THE DISCHARGE

The coefficient of discharge values is shown as an expression of the proportion the head above the crest weir to the height of the weir (H_w/Z) . The illustration shows that the coefficient of the discharge correlates to that combination of (H_w/Z) , as seen in Figures 9, 10 and 11. It indicates that if the curvature angle is substantial, the streamlining lines are linear. However, if it curves, there is a substantial flow velocity, which decreases the discharge coefficient.

Furthermore studied were the effects of height and bending employing several trials. Plotting the mean of the coefficient of discharge (C_d) for every model against elevation (Z) of the weir shows, in Figure 12, that the discharge coefficient climbed as the elevation and curving of the weir rose.

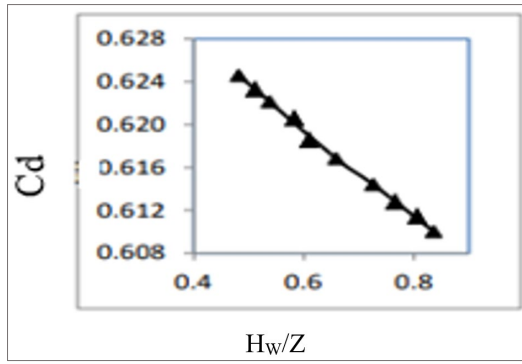


Figure 9. The relationship between discharge coefficient (Cd) and the proportion H_w/Z (Model 1)

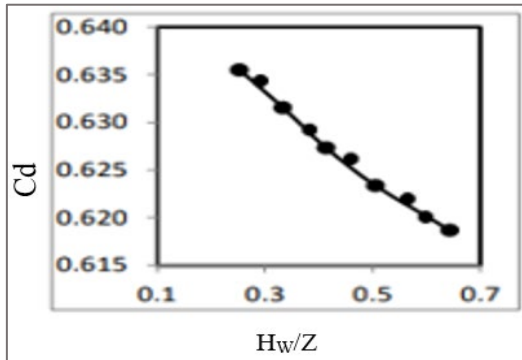


Figure 10. The relationship between discharge coefficient (Cd) and the proportion H_w/Z (Model 2)

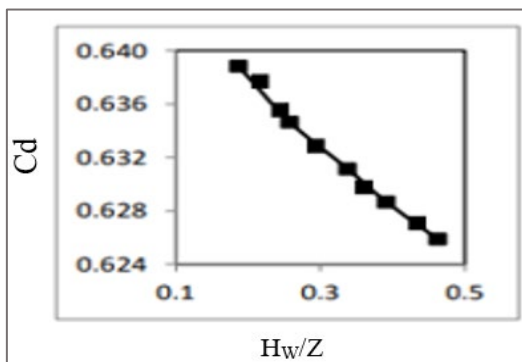


Figure 11. The relationship between discharge coefficient (Cd) and the proportion H_w/Z (Model 3)

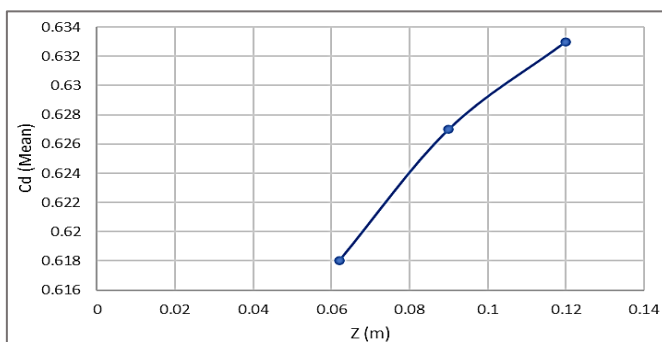


Figure 12. The correlation between the height and discharge coefficient for the three weir models

Discrepancies between theoretical and measured discharges can arise from various factors affecting flow rate predictions'

accuracy. One possible reason is the assumption of ideal flow conditions in theoretical models, which often do not account for real-world complexities such as turbulence, boundary layer effects, and variations in water surface tension. These factors can lead to differences in the actual flow patterns observed in the Flume compared to theoretical predictions.

8. THE FLOW DIMENSIONAL ANALYSIS

There were a lot of different factors that changed the discharge (q) throughout the flow modelling for the rectangular weir. For the flow through a weir, a general expression that does not depend on dimensions is:

$$q = f \left[\frac{Z}{b}, \frac{H_w}{Z}, \frac{H_w}{b}, Cd \right] \quad (13)$$

In order to make predictions regarding the values of (q) to both geometrical and hydraulic parameters, a "multiple nonlinear regression" analysis was utilized, and the Excel program was utilized to complete the analysis. An outstanding counting of the parameter of determinations (R^2) and the error percentage of estimating were generated by the following equation, which was able to match the data:

$$q = A \left(\frac{H_w}{Z} \right) + B \left(\frac{H_w}{b} \right) + C(Cd) + D \left(\frac{Z}{b} \right) \quad (14)$$

where, b is the width of the weir; A, B, C, D are parameters.

The Nash-Sutcliffe model efficiency coefficient (NSE) was used to generate data that fit the findings (experimentally and theoretically). The anticipated accuracy of hydrological simulations is assessed using the Nash-Sutcliffe model efficacy index (NSE), which McCuen et al. [25] proposed. As explicitly stated, it is:

$$NSE = 1 - \frac{\sum_{t=1}^T (Q_o^t - Q_m^t)^2}{\sum_{t=1}^T (Q_o^t - \bar{Q}_o)^2} \quad (15)$$

where, \bar{Q}_o the observed mean discharges, Q_m^t the modelled discharges and Q_o^t is the discharge observed for any time t . The Nash Sutcliffe Efficiency (NSE) resultant is to be equal (1) when the variance error predicting is zero and assumed as a perfected modelling. Conversely, according to Nash and Sutcliffe [26], the Nash-Sutcliffe Efficiency (NSE) value is set to 0 when modelling produces a calculated error variance equal to the observed time series variances. A negative result for the (NSE), shown as NSE less than 0, proposed that the mean observed outperforms the tested model as a predictor. There is a significant agreement between the two sets of findings when the experimental and theoretical findings are compared. A Goodness of Fit (NSE) is displayed in Figures 13(a)-(c). Table 1 displays the coefficients of (A, B, C , and D) to formula 14 for the three models of the weirs together with their corresponding values of R^2 and NSE.

Conducting an error propagation analysis would better assess how uncertainties from various sources—such as instrument precision, environmental factors like temperature, and surface turbulence—impact the results. By quantifying how each factor contributes to the overall uncertainty in flow rate and water level measurements, the analysis would provide a clearer picture of the accuracy and reliability of the experimental outcomes.

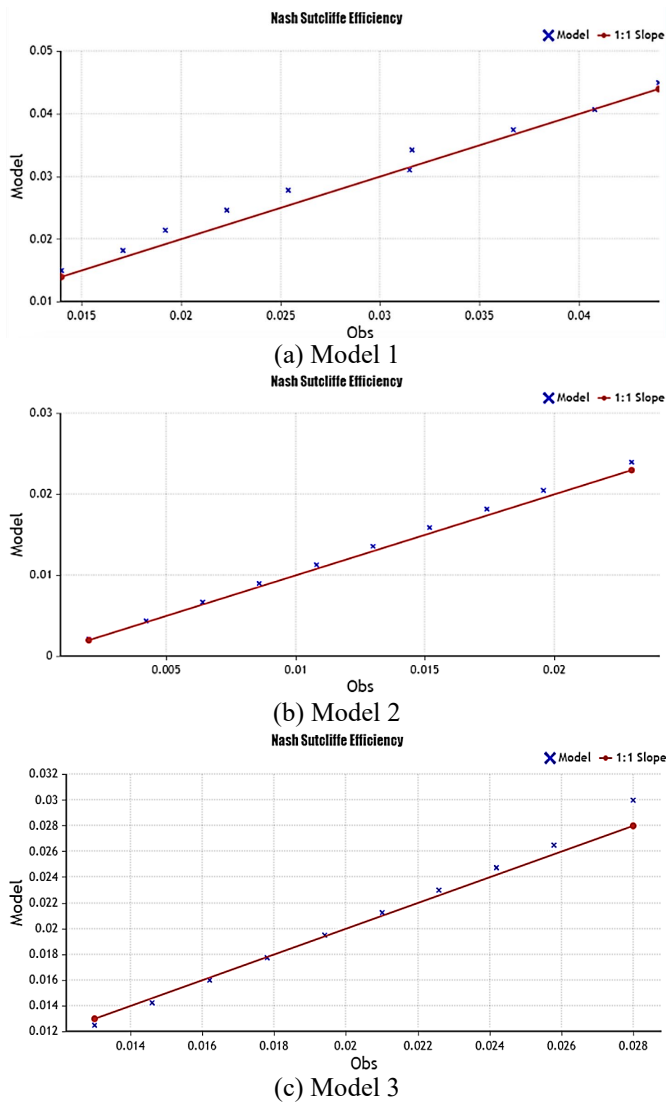


Figure 13. NSE experimental and theoretical models comparisons of the three models

Table 1. The summary findings of the predictive dimensional analysis

Weir	A	B	C	D	NSE	R ²	% Error
Model 1	-2.65	0.35	0.45	-0.16	0.97	0.97	±4
Model 2	-66.23	-25.6	14.01	9.54	0.98	0.98	±2
Model 3	2.45	0.53	-0.21	0.34	0.97	0.99	±4

9. CONCLUSION AND DISCUSSION

The region of accelerating being examined is being confined by centrifugal momentum in both downstream and upstream cross sections, increasing the discharge coefficient and pressure.

In addition to the focus on weir design, this study also explores the instrumentation and measurement techniques critical to the accurate determination of flow rates and water levels. An ultrasonic water level sensor was employed to measure water depth with high precision, addressing challenges such as environmental fluctuations in temperature and humidity, which can affect the speed of sound and thus the sensor's accuracy. To mitigate this, the sensor's built-in temperature compensation feature was utilized, ensuring more reliable readings. Furthermore, turbulent water surfaces posed

a challenge in terms of signal scatter, requiring innovative data smoothing and filtering techniques to achieve consistent measurements. The study also incorporated a real-time data acquisition and logging system, enabling continuous monitoring of water levels and flow rates, which minimized human error and provided a higher resolution of experimental data. The integration of these advanced measurement methods, coupled with robust calibration techniques, enhances the accuracy of the experimental results, contributing valuable insights to the field of instrumentation in hydraulic experiments. The coefficient of discharge (C_d) is significantly influenced by the upward head above the crest (H_w), and the coefficients of discharge decrease as the (H_w) amounts increase over the calibrated range. This is demonstrated by the discharge coefficient (C_d) variance concerning the head normalized to heights and the bend radius (H_w/Z). It should be noted that the downward water level did not affect the flow over the weir, and the results are illustrated in Figure 9. Each of the three systems' heading-discharge equations includes the weir parameter corresponding to the combined value of the approaching head velocity at the measurement point. As a result, the contributions of every value are accounted for in the weir factors (M and K). The permissible intervals for the values of (M) and (K) were provided in Eqs. (10)-(12).

The primary aim of this work is to calculate the coefficient for discharge for a rectangular weir. The laboratory findings, along with the mathematical discharge formula, indicate that the discharge coefficients decrease as the peak of water flowing upstream of the weir crest rises. The level and degree of bend of the overflowing also substantially affect the discharge coefficients (C_d), with parameters increasing as the streamlining bending increases. Therefore, the coefficient of the discharge is contingent upon the dimension and kind of measurement structure.

From real examinations, there were three possible outcomes for (M) and (K), which determined by the geometry of the approach stream segment and the strength of the head that lies over the crested level. The empirically stage-discharge Eqs. (10)-(12) are specific to this structure.

The pattern of pressure changes across the weir surface, and measurements demonstrate that the pressure rises as the head upstream increases.

The multiple determination quadratic regression approach was derived from the observed hydraulic and geometrical parameters, yielding high values for the variance of multiple determinations (R^2) and the standard error of estimate (NSE).

The core focus of this paper is the calibration strategies developed for modified weirs with half-round crest edges. Expanding on this, a detailed comparison with traditional weir calibration methods is essential to highlight the advantages of the proposed approach. Traditional weir calibration often assumes ideal flow conditions, while the modified crest design introduces unique flow patterns that require more precise calibration techniques. By incorporating advanced measurement tools like ultrasonic sensors and real-time data processing, the new calibration strategies offer improved accuracy in flow rate determination, particularly in non-standard flow conditions. This comparison underscores the enhanced performance of the modified weirs and validates the proposed method's superiority over conventional techniques.

In addition to summarizing the main findings, future research should focus on advancing instrumentation and metrology for hydraulic systems. Potential directions include developing more robust sensors for extreme environmental

conditions and integrating machine learning algorithms for real-time flow rate prediction. Expanding the study to encompass various weir geometries and flow conditions could enhance the calibration framework. Improving automation in data acquisition and sensor accuracy in complex flow scenarios will further contribute to the reliability and precision of hydraulic measurements, driving advancements in the field.

REFERENCES

- [1] Nourani, B., Arvanaghi, H., Salmasi, F. (2021). A novel approach for estimation of discharge coefficient in broad-crested weirs based on Harris Hawks Optimization algorithm. *Flow Measurement and Instrumentation*, 79: 101916. <https://doi.org/10.1016/j.flowmeasinst.2021.101916>
- [2] Hamed, M.A. (2023). An experimental study of flow over rectangular broad crested weir. *Engineering Research Journal*, 46(1): 153-158. <https://doi.org/10.21608/ERJM.2022.166247.1217>
- [3] Johnson, M.C. (2000). Discharge coefficient analysis for flat-topped and sharp-crested weirs. *Irrigation Science*, 19: 133-137. <https://doi.org/10.1007/s002719900009>
- [4] Heidarpour, M., Afzalimehr, H., Khorami, E. (2002). Application of stream flow around a circular cylinder to circular-crested weir flow. *JWSS-Isfahan University of Technology*, 6(3): 51-61. <http://dorl.net/dor/20.1001.1.24763594.1381.6.3.4.5>
- [5] Matthew, G.D. (1963). On the influence of curvature, surface tension and viscosity on flow over round-crested weirs. *Proceedings of the Institution of Civil Engineers*, 25(4): 511-524. <https://doi.org/10.1680/iicep.1963.10545>
- [6] Chanson, H. (1996). *Air Bubble Entrainment in Free-Surface Turbulent Shear Flows*. Elsevier.
- [7] Chanson, H., Montes, J.S. (1998). Overflow characteristics of circular weirs: Effects of inflow conditions. *Journal of Irrigation and Drainage Engineering*, 124(3): 152-162. [https://doi.org/10.1061/\(ASCE\)0733-9437\(1998\)124:3\(152\)](https://doi.org/10.1061/(ASCE)0733-9437(1998)124:3(152))
- [8] Ramamurthy, A.S., Qu, J., Zhai, C., Vo, D. (2007). Multislit weir characteristics. *Journal of Irrigation and Drainage Engineering*, 133(2): 198-200. [https://doi.org/10.1061/\(ASCE\)0733-9437\(2007\)133:2\(198\)](https://doi.org/10.1061/(ASCE)0733-9437(2007)133:2(198))
- [9] Jalil, S.A., Ibrahim, S.S., Jafer, R.A. (2014). Research article surface roughness effects on discharge coefficient of broad crested weir. *Research Journal of Applied Sciences, Engineering and Technology*, 7(24): 5227-5233. <https://doi.org/10.19026/rjaset.7.918>
- [10] Al Bayaty, M.A. (2024). Detection and analysis the change in LULC in some riparian area of euphrates river through using land sat data and GIS technique. *Instrumentation Measure Métrologie*, 23(4): 329-338. <https://doi.org/10.18280/i2m.230408>
- [11] Isleem, H.F., Elshaarawy, M.K., Hamed, A.K. (2024). Analysis of flow dynamics and energy dissipation in piano key and labyrinth weirs using computational fluid dynamics. In *Computational Fluid Dynamics - Analysis, Simulations, and Applications*. <https://doi.org/10.5772/intechopen.1006332>
- [12] Castro-Orgaz, O. (2008). Curvilinear flow over round-crested weirs. *Journal of Hydraulic Research*, 46(4): 543-547. [https://doi.org/10.1061/\(ASCE\)0733-9437\(1998\)124:3\(152\)](https://doi.org/10.1061/(ASCE)0733-9437(1998)124:3(152))
- [13] Kumar, S., Ahmad, Z., Mansoor, T., Himanshu, S.K. (2012). Discharge characteristics of sharp crested weir of curved plan-form. *Research Journal of Engineering Sciences*, 1(4): 16-20. <https://www.isca.me/IJES/Archive/v1/i4/3.ISCA-RJEngS-2012-066.pdf>
- [14] Haghiabi, A.H. (2012). Hydraulic characteristics of circular crested weir based on Dressler theory. *Biosystems Engineering*, 112(4): 328-334. <https://doi.org/10.1016/j.biosystemseng.2012.05.004>
- [15] Hamad Mohammed, R. (2013). Calibrating the discharge coefficient of rectangular with quarter circular edge crested weir. *Journal of Kerbala University*, 11(2): 64-73. <https://www.iasj.net/iasj/article/76642>
- [16] Bazin, H.É. (1898). *Experiences Nouvelles Sur L'écoulement En Deversoir: Exécutes a Dijon de 1886 a 1895*. Dunod.
- [17] Salmasi, F., Sabahi, N., Abraham, J. (2021). Discharge coefficients for rectangular broad-crested gabion weirs: Experimental study. *Journal of Irrigation and Drainage Engineering*, 147(3): 04021001. [https://doi.org/10.1061/\(ASCE\)IR.1943-4774.0001535](https://doi.org/10.1061/(ASCE)IR.1943-4774.0001535)
- [18] Alfatlawi, T.J.M., Hussein, A.H. (2024). A numerical study of diversion flow to determine the optimum flow system in open channels. *Water Practice & Technology*, 19(4): 1330-1347. <https://doi.org/10.2166/wpt.2024.056>
- [19] Williams, M.L. (1993). *Calibration of Long Crested Weir Discharge Coefficient*. University of Wyoming.
- [20] Yang, J., Li, S., Helgesson, A., Skepparkrans, E., Ansell, A. (2023). Geometric modification of piano key weirs to enhance hydraulic performance and discharge capacity. *Water*, 15(23): 4148. <https://doi.org/10.3390/w15234148>
- [21] Zerihun, Y.T. (2020). Free flow and discharge characteristics of trapezoidal-shaped weirs. *Fluids*, 5(4): 238. <https://doi.org/10.3390/fluids5040238>
- [22] Hussein, A.H., Al-Delewy, A.A., Nasir, M.J. (2018). Estimating the capability of Shatt Al-Hilla within Hilla City to carry the total bed-material load. In *International Conference on Materials Engineering and Science*, Istanbul, Turkey, 454(1): 012020. <https://doi.org/10.1088/1757899X/454/1/012020>
- [23] Berger, R.C., Carey, G.F. (1998). Free-surface flow over curved surfaces: Part II: Computational Model. *International Journal for Numerical Methods in Fluids*, 28(2): 201-213. [https://doi.org/10.1002/\(SICI\)1097-0363\(19980815\)28:2%3C201::AID-FLD706%3E3.0.CO;2-Q](https://doi.org/10.1002/(SICI)1097-0363(19980815)28:2%3C201::AID-FLD706%3E3.0.CO;2-Q)
- [24] Alfatlawi, T.J., Hussein, A.H. (2024). A review of studying the flow characteristics in branching open channels. *International Journal of Heat and Technology*, 42(2): 560-566. <https://doi.org/10.18280/ijht.420222>
- [25] McCuen, R.H., Knight, Z., Cutter, A.G. (2006). Evaluation of the Nash-Sutcliffe efficiency index. *Journal of Hydrologic Engineering*, 11(6): 597-602. [https://doi.org/10.1061/\(ASCE\)1084-0699\(2006\)11:6\(597\)](https://doi.org/10.1061/(ASCE)1084-0699(2006)11:6(597))
- [26] Nash, J.E., Sutcliffe, J.V. (1970). River flow forecasting through conceptual models part I—A discussion of principles. *Journal of Hydrology*, 10(3): 282-290. [https://doi.org/10.1016/0022-1694\(70\)90255-6](https://doi.org/10.1016/0022-1694(70)90255-6)